

# Parametric Analysis of Response Function in Modeling Combustion Instability by a Quasi-1D Solver

**M. L. Frezzotti and F. Nasuti**

*Sapienza, University of Rome, via Eudossiana 18, 00184, Rome, Italy  
marialuisa.frezzotti@uniroma1.it, francesco.nasuti@uniroma1.it*

**C. Huang, C. Merkle and W. E. Anderson**

*Purdue University, 701 W. Stadium Ave., West Lafayette, IN, 47907, USA  
huang162@purdue.edu, merkle@purdue.edu, wanderso@purdue.edu*

## Abstract

A parametric study of the CVRC combustor test case is carried out by a quasi-1D Eulerian solver including a pressure lag response function which is used to take into account the unsteady heat release, typically driving combustion instability phenomena. The parameters under investigation are those defining the selected response function that are its amplitude and characteristic time lag. Both stable and unstable cases have been obtained for a wide range of amplitude and time lag which allow to investigate limit cycles at moderate amplitude. The extension of the approach to even higher amplitude of limit cycles of the order of those actually obtained in CVRC is presently in progress.

## 1. Introduction

Combustion instability results from the coupling between unsteady heat release and pressure oscillations that is established through a feedback path. Despite the many years of research in the subject, no proven a priori predictive method is known, posing high risks during development of new systems.

High fidelity models like large eddy simulations (LES) and hybrid RANS-LES simulations<sup>1-7</sup> have been successfully applied in the past years. The computational cost associated to these kind of numerical simulations can be partially limited introducing simplificative assumptions, such as reduced mechanisms for chemical kinetics or axisymmetry hypothesis,<sup>1,7</sup> when possible. Other simplifications can be introduced for describing the boundary conditions<sup>8</sup> but of course this is a very delicate aspect. In fact it is well known that the choice of improper boundary conditions can lead to quite inaccurate results.<sup>9</sup>

Generally speaking, several assumptions can be introduced to decrease the computational cost, but sometimes they can have detrimental effects on the results reliability and it is also noteworthy that the benefit, in terms of time and computational resources, even if considerable, does not allow to completely overcome the problem. As a result, in most cases, the high fidelity models are prohibitive in terms of computational effort to be considered as an option during the design phase of a new engine. For this reason, improvement and development of reliable reduced models is still a mandatory task.

In the past years, linear models have been widely studied but their intrinsic limitation in studying the combustion instability problem is quite evident, considering the role that nonlinearities have in limit cycle development. The objective of the present work is to evaluate the potential and the limitations of a quasi-1D Eulerian solver (Q1DEE) that is able to take into account the nonlinearities due to acoustics. In previous works it has been shown that the solver is capable of identifying resonant frequencies and modal shapes with reasonable approximation.<sup>10,11</sup> The main difficulty in considering a low order model, such as the Euler quasi-1D formulation, consists in the necessity of modeling the coupling between unsteady heat release and acoustics providing a suitable response function, i.e. a formulation of unsteady heat release as a function of other variables, like pressure or velocity. Several formulations of response functions have been proposed and a summary of the various forms is given by Portillo et al<sup>12</sup> in both time and frequency domain.

In the present work the solver capability in capturing the nonlinear behavior in a single element combustor, the continuous variable resonance combustor (CVRC),<sup>13</sup> with the combined use of the quasi-1D Eulerian model and a pressure lag response function, is investigated through a parametric study.

## 2. The CVRC Test Case

The test case is the CVRC experiment, realized and installed at Purdue University with the main aim to investigate the effect that the oxidizer post length can have on instability. Propellants are hydrogen peroxide, dissociated in  $H_2O$  and  $O_2$  on a catalyst bed, and methane, injected through a single coaxial injector. The characteristic feature of CVRC is the presence of an actuator that is able to continuously vary the length of the oxidizer post. In the present study a fixed oxidizer post length configuration (0.1397 m) is considered. This single element combustor has been widely studied through a number of experiments and simulations.<sup>2,7,14–18</sup> The average operating conditions are summarized in Table 1 while Fig. 1 is a sketch of the computational domain where the main components are labeled.

Table 1 – CVRC operating conditions.

Parameter	Value
Fuel Mass Flow Rate, kg/s	0.027
Fuel Temperature, K	300
Oxidizer Mass Flow Rate, kg/s	0.32
Oxidizer Temperature, K	1030
Mass Fraction $H_2O$ , %	57.6
Mass Fraction $O_2$ , %	42.4
Equivalence Ratio	0.8

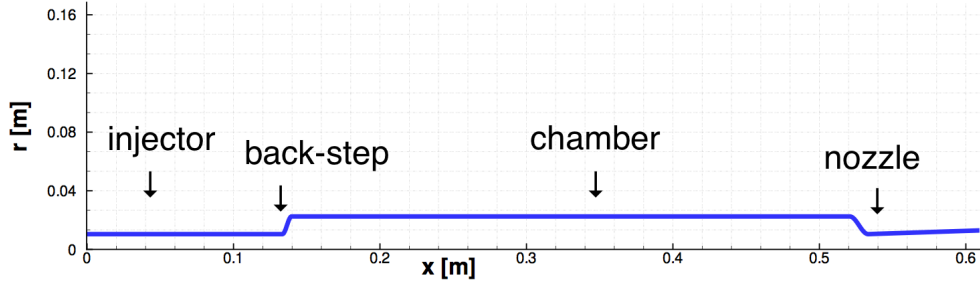


Figure 1 – Geometry of CVRC.

## 3. Quasi-1D Eulerian Solver

In the present section a brief overview of the solver is given. For further details, see Smith et al.,<sup>11</sup> Sankaran et al.<sup>19</sup> and Buelow et al.<sup>20</sup>

The governing equations are written as

$$\frac{\partial Q}{\partial t} + \frac{\partial E}{\partial x} = H + H_f + H_q \quad (1)$$

where

$$Q = \begin{pmatrix} \rho A \\ \rho u A \\ \rho e_0 A \\ \rho Y_{ox} A \end{pmatrix} \quad E = \begin{pmatrix} \rho u A \\ (\rho u^2 + p) u A \\ [\rho u (e_0 + \frac{p}{\rho})] A \\ \rho u Y_{ox} A \end{pmatrix} \quad H = \begin{pmatrix} 0 \\ p \frac{dA}{dx} \\ 0 \\ 0 \end{pmatrix} \quad H_f = \begin{pmatrix} \dot{\omega}_f A \\ \dot{\omega}_f u A \\ \dot{\omega}_f h_0 A \\ -\dot{\omega}_{ox} A \end{pmatrix} \quad H_q = \begin{pmatrix} 0 \\ 0 \\ q' \\ 0 \end{pmatrix} \quad (2)$$

The source term on the right hand side has been split in three different contributions:  $H$ ,  $H_f$  and  $H_q$ . The first source term,  $H$ , is the term due to area variations while the other two terms are related to combustion. More specifically,  $H_f$  represents the mean source term for combustion, where only two species have been considered: the oxidizer and the combustion products, the latter computed with CEA.<sup>21</sup> In fact, the main assumption is that fuel reacts instantaneously to form products with the main consequence of neglecting intermediate species and finite reaction rates. Combustion is described as consumption of oxidizer which is replaced by combustion products with the proportion

$$\dot{\omega}_f = C_{f/o} \dot{\omega}_{ox} \quad (3)$$

The oxidizer is therefore introduced at the boundary, while the combustion products, or equivalently the fuel as it reacts immediately, are introduced in a region near the interface between the oxidizer post and the combustion chamber referred as back-step or dump-plane. In order to avoid discontinuities and to reproduce a combustion region of finite length, the combustion products injection rate spans, for the case of CVRC, the region between the two abscissas,  $l_s = 0.1334 \text{ m}$  and  $l_f = 0.2096 \text{ m}$  (Fig. 1), and is shaped like a sinusoid, yielding

$$\dot{\omega}_{ox} = k_f \rho Y_{ox} (1 + \sin \xi) \quad (4)$$

$$\text{with } \xi = -\frac{\pi}{2} + 2\pi \frac{x - l_s}{l_f - l_s} \quad \text{for } l_s < x < l_f \quad (5)$$

The reaction constant  $k_f = 1.72 \cdot 10^4 \text{ Hz}^{-1}$  is selected in order to assure that only combustion products are present downstream the prescribed combustion region.

The last contribution,  $H_q$ , refers to the unsteady heat release term. It represents the response function through which the model takes into account coupling between acoustics and combustion. This is performed, expressing the unsteady part of heat release as function of pressure, with a certain time lag  $\tau$

$$q'(x, t) = \frac{e^{-\frac{(x-\mu)^2}{2\sigma^2}}}{\sqrt{2\pi\sigma^2}} \alpha A(x) [p(x, t - \tau) - \bar{p}(x)]. \quad (6)$$

In order to avoid discontinuities, the unsteady heat release rate is distributed in the domain, following a Gaussian distribution characterized by  $\sigma = 0.0141 \text{ m}$  and  $\mu = 0.1797 \text{ m}$ . The value of  $\mu$  has been selected on the basis of the results of CFD simulations showing that it is the position where unsteady heat release is maximum. The axial position is almost centered with respect to the steady combustion region. As can be seen looking at Section 2, where the geometry of CVRC is described, the distribution is placed just downstream the back-step between the injector and the chamber (Fig. 2).

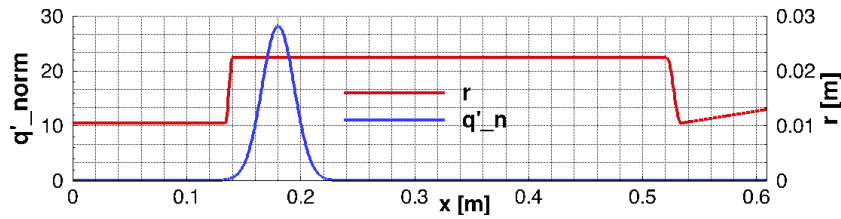


Figure 2 – Geometry of CVRC and normalized distribution of unsteady heat release.

The proportionality between pressure oscillation at a previous time step ( $t - \tau$ ) and heat release is established through the Gaussian distribution and the constant  $\alpha$ . The parametric study is carried out varying the two parameters  $\alpha$  and  $\tau$ .

In order to have a correct interpretation of the results presented in the following sections, it is necessary to briefly describe the procedure used to obtain the pressure behavior for a given response function. First of all, the steady state solution is computed and its consistency with the data available in literature is verified. Then, the resonant frequencies are identified applying a broadband disturbance on the oxidizer mass flow rate. A single frequency disturbance of small amplitude and of frequency corresponding to the chamber first longitudinal mode, is then applied to the mass flow rate until the pressure starts oscillating between two fixed values (0.04 s is a sufficient time in this case). At this point, the disturbance is turned off and, at the same time, the response function is activated.

For the present test case the considered pressure signals correspond to the values registered at  $x = 0.5080 \text{ m}$ , that is close to the dump-plane. The choice of the point is related to the presence of a pressure probe at this abscissa in the experimental test. Moreover, the selected position is close to the pressure antinode for the chamber longitudinal modes.

The combustor has been modeled as a quasi-1D domain, represented in Fig. 1. The grid consists of 1200 nodes (constant  $\Delta x$ ). The number of nodes has been chosen on the basis of a grid convergence study.

For the sake of brevity, only the comparison between the steady state results is shown (Fig. 3) and summarized in Table 2 where the pressure computed with the two coarser grids for a fixed abscissa ( $x = 0.50 \text{ m}$ ) are compared with the pressure value obtained with the finer grid. The computed error ( $\epsilon \leq 0.2\%$ ) justifies the choice of the coarser grid. The associated time step is  $\Delta t = 2\mu\text{s}$ .

Table 2 – Grid convergence study. The pressure values in the table correspond to the steady state values computed for  $x = 0.50 \text{ m}$

Nodes	Pressure [MPa]	Error %
4800	1.53393	—
2400	1.53312	0.05
1200	1.53087	0.20

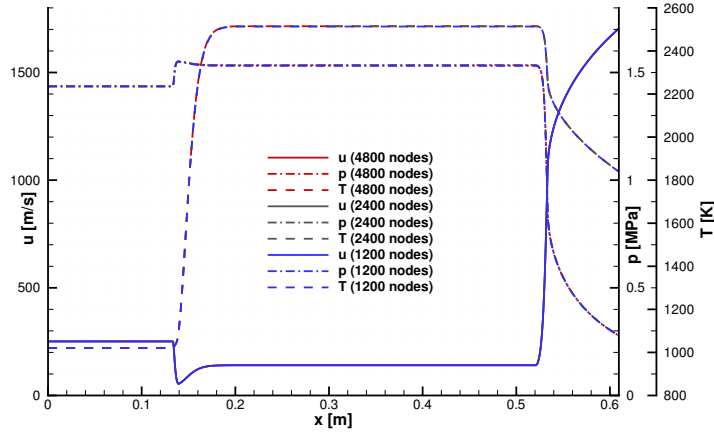


Figure 3 – Steady state solution. Comparison between three different grids.

## 4. Results

As briefly explained in Section 3, in order to test different response functions it is necessary to compute the steady state solution (see Fig. 3) and the resonant frequencies first. Table 3 summarizes the values of the first three longitudinal frequencies. Comparing experimental and numerical data it is possible to conclude that the Q1DEE is able to estimate the resonant frequencies with reasonable approximation as already known from previous works.<sup>10,11</sup>

Table 3 – CVRC resonant frequencies. Comparison between computed<sup>22</sup> and experimental values

Mode	Computed Frequency [Hz]	Experimental Frequency [Hz]	Error %
1L	1400	1330	5.3
2L	2700	2660	1.5
3L	4200	3990	5.3

The parametric study has been carried out considering three different values for the parameter  $\tau/T$  where  $T$  is the time period associated to the first longitudinal resonant frequency: 0.93, 0.85, 0.7.

Figure 4 shows the results obtained for different values of  $\alpha$  with  $\tau/T = 0.85$ . As expected, increasing the  $\alpha$  value, the amplitude of the limit cycle and the growth rate increase too. For  $\alpha \geq 1300 \text{ m/s}$  an overshoot can be observed. Focusing on the limit cycle it can be noticed that the cycle is not symmetric with respect to the initial average value (i.e. the steady state value). Moreover, Fig. 5a shows the pressure signal at the axial position  $x = 0.5080 \text{ m}$ . A peculiar characteristic, observed both in the experiments and in high fidelity simulations, is the presence of a steep front that in this case is not very developed suggesting a weak nonlinearity. Figure 5b is a zoom on the growing phase of the signal. The peaks envelope at the beginning of the growth, follows an exponential curve in agreement with the linear theory.

Figure 6 shows an example of decay obtained with  $\alpha = 1100 \text{ m/s}$  and  $\tau/T = 0.85$ . As anticipated, even if the response function is activated, the energy introduced with the unsteady heat release  $q'$  is not sufficient to sustain instability. In fact, even if the  $\tau/T$  parameter is suitable for driving instability according to the Rayleigh criterion, (releasing the heat during the compression), the energy loss due to entropy waves that leave the domain through the nozzle is able to prevent instability, exerting a damping effect that increases with the flow Mach number.

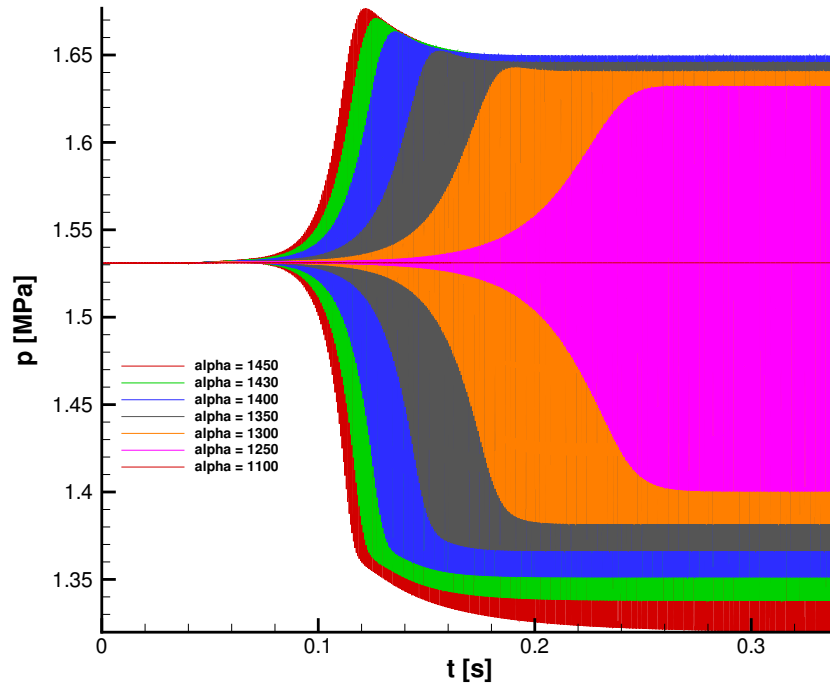
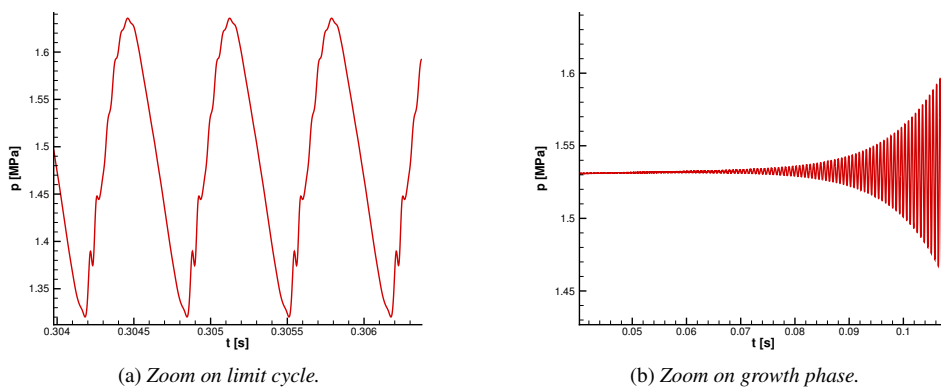


Figure 4 – Unsteady computations for  $\alpha \leq 1400 \text{ m/s}$  and  $\tau/T = 0.85$



(a) Zoom on limit cycle.

(b) Zoom on growth phase.

Figure 5 – Unsteady computation for  $\alpha = 1450 \text{ m/s}$  and  $\tau/T = 0.85$ .

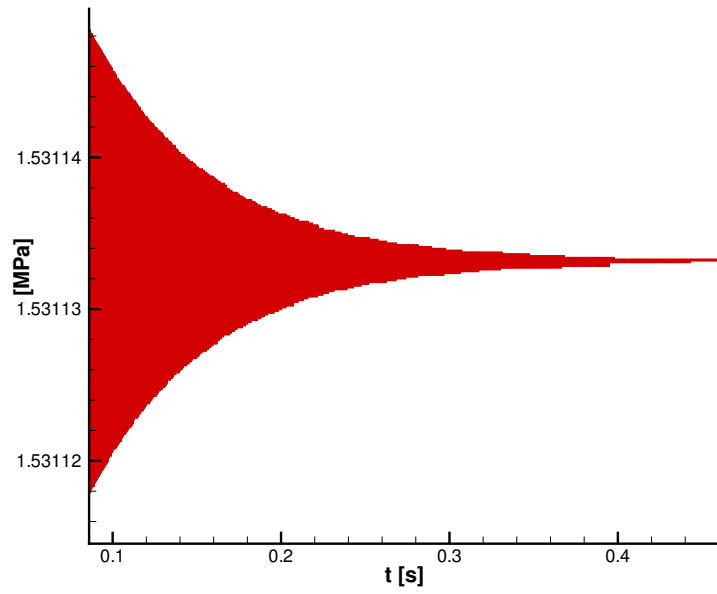


Figure 6 – Pressure signal for  $\alpha = 1100 \text{ m/s}$  and  $\tau/T = 0.85$  at  $x = 0.5080 \text{ m}$

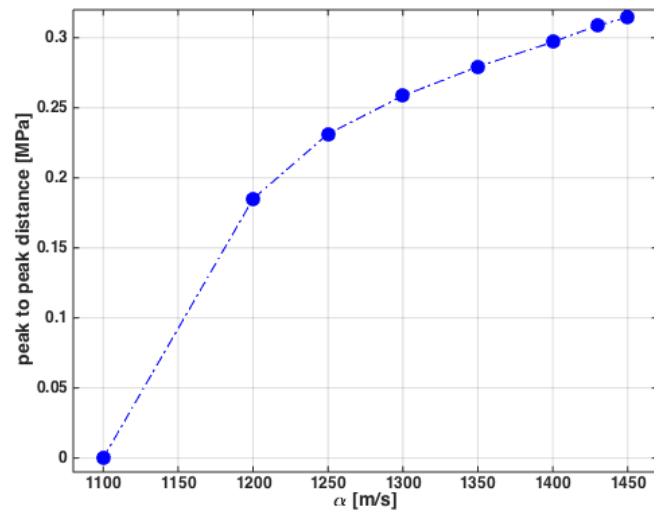


Figure 7 – Peak to peak distance for  $\tau/T = 0.85$  varying the  $\alpha$  value

One of the very basic objectives in the simulation is to match the limit cycle amplitude in order to verify if the pressure oscillations can be tolerated by the system. For this reason Fig. 7 shows the peak to peak distance at limit cycle for different  $\alpha$  values ( $\tau/T = 0.85$ ). The results are distributed along a monotonically growing curve characterized by a decreasing derivative. Figure 8 shows the peak to peak distance as a function of  $\tau/T$  where  $\alpha$  is a parameter.

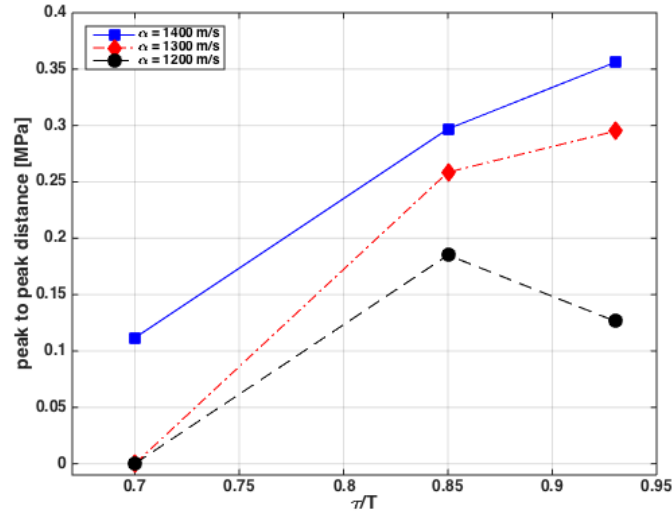


Figure 8 – Peak to peak distance for several values of  $\tau/T$  and  $\alpha$

As expected, the amplitude of limit cycle grows with growing values of  $\alpha$  and with  $\tau/T$  approaching 1. The only exception to this behavior is represented by the case  $\alpha = 1200$  m/s,  $\tau/T = 0.93$ .

With the available data it is possible to plot the stability map in Fig. 9. The dash-dotted line represents the lower limit of the unstable region while the solid one is the upper limit of the stable zone. Of course, the area of the transition region can be progressively reduced considering  $\alpha$  values within the range established by the upper and lower limit.

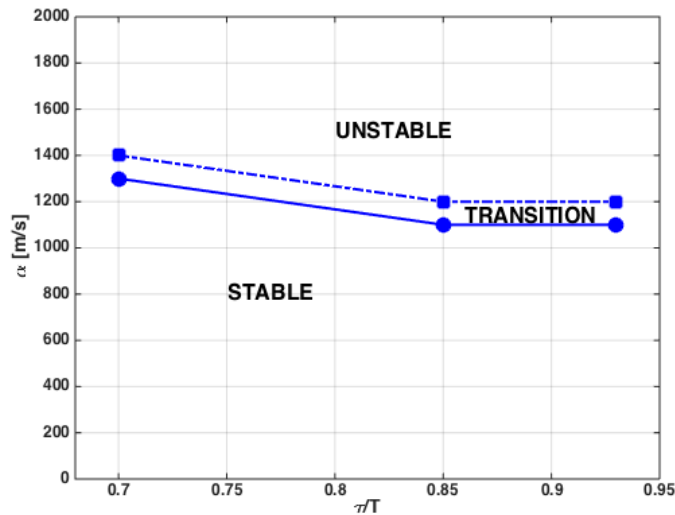


Figure 9 – Stability map. The transition region is identified by the upper and lower limit, dash-dotted and solid line respectively.

The amplitude of limit cycle explored so far, with  $\alpha$  values up to 1400 m/s, is quite low if compared with experimental and numerical data available in literature (see for example Harvazinski,<sup>1</sup> Harvazinski et al.<sup>2</sup> or Sardeshmukh et al.<sup>7</sup>). Moreover, at present the solver has not been able to deal with larger  $\alpha$  because of the intensity of waves that have posed some modeling numerical issues. One of the encountered difficulties is connected to the role of average

pressure in eq. (6). In fact, in eq. (6) the unsteady heat release is proportional to the difference  $[p(x, t - \tau) - \bar{p}(x)]$  where  $\bar{p}(x)$  represents the steady state solution. This is in contrast with the intrinsic nonlinearity of the solver. Assuming that it is possible to split the pressure in an average part, fixed in time and coincident with the steady state solution, and an oscillating part, we are assuming that it is possible to apply the superimposition of the effects, while this is not the case for nonlinear problems. During the unsteady computation the mean pressure can be shifted but this shift is not considered in the unsteady heat release computation that is referred to pressure steady state value at the given abscissa. As a consequence, if the mean pressure value changes, the heat release will be decreased or increased by a fixed quantity, proportional to the difference between the steady state value and the new mean pressure value. The variation in the average heat release produces a variation in the mean temperature and, consequently, in resonant frequencies and corresponding time period  $T$ . On the contrary,  $\tau$  is an input parameter and consequently  $\tau/T$  changes causing the damping of pressure oscillations.

## 5. Conclusions

A numerical parametric study has been carried out on the CVRC test case by a quasi-1D Eulerian solver, where the unsteady heat release is taken into account considering a pressure lag response function characterized by two parameters:  $\tau/T$  and  $\alpha$ . In particular, three values of  $\tau/T$  have been considered: 0.7, 0.85, 0.93. Both stable and unstable cases have been obtained depending on the  $\tau/T$  and  $\alpha$  values. In particular, it has been shown that the peak to peak distance at limit cycle for pressure signal increases if  $\tau/T$  approaches 1 or if  $\alpha$  grows. Nevertheless the increase of  $\alpha$  is possible up to a certain limit that does not allow to reach the peak to peak distance characterizing the CVRC experimental pressure oscillations. The fundamental limitation consists in the response function formulation. In fact the splitting of pressure into a fix, average part, coincident with the steady state value, plus an oscillating part, is successfully applied in linear or weakly nonlinear regime while it fails in nonlinear problems, characterized by pressure oscillations of higher intensity. In fact the pressure average value does not coincides with the steady state value. For this reason, aiming to analyze the behavior at higher values of  $\alpha$  which would yield pressure oscillations of the same amplitude as shown by experiments, a different formulation of response function, capable of taking into account the nonlinearity of the problem, should be explored.

## Acknowledgment

The authors want to acknowledge Dr. V. Sankaran for his suggestions.

## References

- [1] Harvazinski, M. E., *Modeling of self-excited combustion instabilities using a combination of two- and three-dimensional simulations*, Ph.D. thesis, Purdue University, 2012.
- [2] Harvazinski, M. E., Huang, C., Sankaran, V., Feldman, T. W., Anderson, W. E., Merkle, C. L., and Talley, D. G., "Combustion Instability Mechanisms in a Pressure-coupled Gas-gas Coaxial Rocket Injector," 2013, 49th AIAA/ASME/SAE/ASEE Joint Propulsion Conference, July, San Jose, CA.
- [3] Chong, L. T. W., Bomberg, S., Ulhaq, A., Komarek, T., and Polifke, W., "Comparative Validation Study on Identification of Premixed Flame Transfer Function," *Journal of Engineering for Gas Turbines and Power, Volume 134*, 2012.
- [4] Chong, L. T. W., Kaess, R., Komarek, T., Foller, S., and Polifke, W., "Identification of Flame Transfer Function from LES of Turbulent Reacting Flows," 2009, High Performance Computing in Science and Engineering, Garchin/Munich pp. 255-266.
- [5] Krediet, H. J., Beck, C. H., Krebs, W., Schimek, S., Paschereit, C. O., and Kok, J. B. W., "Identification of the Flame Describing Function of a Premixed Swirl Flame from LES," *Combustion Science and Technology, vol. 184, pp. 888-900*, 2012.
- [6] Chong, L. T. W., Komarek, T., Kaess, R., Foller, S., and Polifke, W., "Identification of Flame Transfer Function from LES of a Premixed Swirl Burner," 2010, ASME Turbo Expo 2010: Power for Land, Sea and Air, June 14-18, Glasgow, UK.
- [7] Sardeshmukh, S. V., Anderson, W. E., Harvazinski, M. E., and Sankaran, V., "Prediction of Combustion Instability with Detailed Chemical Kinetics," 53th AIAA Aerospace Science Meeting, January 2015, Kissimmee, FL.



- [8] Harvazinski, M. E., Talley, D. G., and Sankaran, V., "Influence of Boundary Condition Treatment on Longitudinal Mode Combustion Instability Predictions," 2013, 49th AIAA/ASME/SAE/ASEE Joint Propulsion Conference, July, San Jose, CA.
- [9] Garby, R., Selle, L., and Poinso, T., "Analysis of the Impact of Heat Losses on an Unstable Model Rocket-Engine Combustor Using Large Eddy Simulation," 48th AIAA/ASME/SAE/ASEE Joint Propulsion Conference & Exhibit, 30 July-01 August 2012, Atlanta, Georgia.
- [10] Frezzotti, M. L., Terracciano, A., Nasuti, F., Hester, S., and Anderson, W. E., "Low-order model studies of combustion instability in a DVRC combustor," 2014, 50th AIAA/ASME/SAE/ASEE Joint Propulsion Conference, July, Cleveland, OH.
- [11] Smith, R., Ellis, M., Xia, G., Sankaran, V., Anderson, W., and Merkle, C. L., "Computational Investigation of Acoustics and Instabilities in a Longitudinal-Mode Rocket Combustor," *AIAA Journal*, Vol. 46, No. 11, November, 2008.
- [12] Portillo, J. E., Sisco, J. C., Corless, M. J., Sankaran, V., and Anderson, W. E., "Generalized Combustion Instability Model," 2006, 42nd AIAA/ASME/SAE/ASEE Joint Propulsion Conference, July, Sacramento, CA.
- [13] Yu, Y. C., Koeglmeier, S. M., Sisco, J. C., Smith, R. J., and Anderson, W. E., "Combustion Instability of Gaseous Fuels in a Continuously Variable Resonance Chamber (CVRC)," 2008, 44th AIAA/ASME/SAE/ASEE Joint Propulsion Conference & Exhibit, July, Hartford, CT.
- [14] Garby, R., *Simulations of Flame Stabilization and Stability in High-Pressure Propulsion Systems*, Ph.D. thesis, Université de Toulouse, Institut National Polytechnique de Toulouse, 2013.
- [15] Yu, Y. C., O'Hara, L., Sisco, J. C., and Anderson, W. E., "Examination of Mode Shapes in an Unstable Model Rocket Combustor," 2009, 47th AIAA Aerospace Sciences Meeting Including the New Horizons Forum and Aerospace Expositions, 5-8 January, Orlando, Florida.
- [16] O'Hara, L., Yu, Y., Smith, R. J., Anderson, W. E., and Merkle, C., "Investigations to an Unsteady Heat Release Model Applied to an Unstable Liquid Rocket Combustor," 2009, 45th AIAA/ASME/SAE/ASEE Joint Propulsion Conference & Exhibit, 2-5 August, Denver, Colorado.
- [17] Sisco, J. C., Portillo, J. E., Yu, Y. C., and Anderson, W. E., "Non-Linear Characteristic of Longitudinal Instabilities in a Model Rocket Combustor," 2007, 43rd AIAA/ASME/SAE/ASEE Joint Propulsion Conference & Exhibit, 8-11 July, Cincinnati, OH.
- [18] Yu, Y. C., Sisco, J. C., and Anderson, W. E., "Examination of Spatial Mode Shapes and Resonant Frequencies Using Linearized Euler Solutions," 2007, 37th AIAA Fluid Dynamic Conference & Exhibit, 25-28 June, Miami, FL.
- [19] Sankaran, V. and Merkle, C. L., "Dual Time Stepping and Preconditioning for Unsteady Computations," 33th AIAA Aerospace Science Meeting and Exhibit, January 1995, Reno, NV.
- [20] Buelow, P. E. O., Schwer, D. A., Feng, J., Merkle, C. L., and Choi, D., "A Preconditioned Dual Time, Diagonalized ADI Scheme for Unsteady Computations," 13th Computational Fluid Dynamics Conference, 1995, Snowmass Village, CO.
- [21] McBride, B. J. and Gordon, S., "Computer Program for Calculation of Complex Chemical Equilibrium Compositions and Applications," Tech. Rep. 1311, 1994, NASA Reference Publication.
- [22] Yu, Y. C., Sisco, J. C., Rosen, S., Madhav, A., and Anderson, W. E., "Spontaneous Longitudinal Combustion Instability in a Continuously-Variable Resonance Combustor," *Journal of Propulsion and Power*, Vol. 28, pp. 876-887, 2012.